J. Chem. Sci. (2022) 134:25
https://doi.org/10.1007/s12039-021-02014-0

REGULAR ARTICLE

Role of the weak noncovalent interactions in the stability of the aggregated protonated dopamine in the aqueous solution: spectroscopic and quantum chemical calculation studies

ABHINANDA CHOWDHURY and PRASHANT CHANDRA SINGH*
School of Chemical Sciences, Indian Association for the Cultivation of Science, Jadavpur, Kolkata 700032, India
E-mail: sppcs@iacs.res.in

MS received 20 September 2021; revised 21 October 2021; accepted 21 October 2021

Abstract. The conformational state and noncovalent interaction of protonated dopamine (p-dopamine) play an important role in its key and lock binding with its receptors. Hence, understanding of the role of weak noncovalent interactions in the stability of the higher order structures of the p-dopamine is desired. In this study, we have combined the spectroscopic and quantum chemical calculation studies to understand the role of noncovalent interactions in the stability of the dimers and trimers of p-dopamine in the aqueous medium. The intensity of the UV–Visible spectra of p-dopamine increases and shows a red shift with increasing concentrations suggesting the presence of the higher order structures of p-dopamine in the aqueous medium. The quantum chemical calculations and AIM studies of the different structures of its dimer and trimers suggest the presence of $N–H_3^{+}\cdots\pi$, $C–H\cdots\pi$, $\pi\cdots\pi$ weak interactions along with conventional $N–H\cdots O$ hydrogen bond. The calculated peak positions of the UV–Visible spectra of different clusters show that the higher order of clusters show red shifted peak position compared to the monomer and the red shifted peak is more evident in the clusters having noncovalent interactions.

Keywords. Protonated dopamine; noncovalent intercations; UV–visible spectra; higher order clusters; red shift; quantum chemical calculations.

1. Introduction

Dopamine is an important neurotransmitter which belongs to the catecholamine and phenethylamine families and acts as a hormone in the central and peripheral nervous systems.[1–4] Synthesised from the precursor L-DOPA, it is the main ligand for dopaminergic pathways of the brain which are involved in arousal and reward-motivated behaviour.[5–8] The dysfunction of dopamine is related to neurological disorders like Parkinson's disease, and schizophrenia.[9–11] Dopamine has high flexibility and conformational variety due to the possible rotations around the C–N and C–C bonds of the aminoethyl side chain. Dopamine has a flexible side chain with amine group which provides the possibility of weak noncovalent interactions and affects the stability of its conformational state.[12–15] Extensive efforts have been devoted to study the conformations of dopamine in various media.[16–21] One rotational study of the neutral dopamine shows that the gauche form of dopamine is most stable in the gas phase.[12] This study depicts the possibility of the existence of seven different conformers of dopamine in the gas phase and the stability of these rotamers is strongly influenced by $N–H_3^{+}\cdots\pi$ interaction.

It is well known that dopamine exists in the protonated form ($-NH_2$ of dopamine gets protonated) at the physiological pH $\sim$7.4.[22,23] Indeed, the X-ray crystal structure of dopamine shows that the protonated form is more stabilized than the neutral form which is also supported by the NMR and IR data.[20,24] The pH dependent NMR study of the protonated dopamine (further referred to as p-dopamine) suggests that the *gauche* form of the aminoethyl side chain with respect to the aromatic moiety is more favourable than the *trans* form in the acidic condition, whereas, the *trans* form takes over the *gauche*

*For correspondence

Supplementary Information: The online version contains supplementary material available at https://doi.org/10.1007/s12039-021-02014-0.

Published online: 05 February 2022

conformation of p-dopamine in the basic condition.[24] In one of the theoretical studies, it has also been suggested that the hydrogen bonding of the solvent stabilizes the *anti* conformers of p-dopamine and the stability of this form is similar to the conformer with the intramolecular hydrogen bond.[25] In the gas phase study of p-dopamine, it has been reported that the *gauche* form of dopamine is more stable than the *trans* form and the $–NH_2$ group is pointing towards the benzene ring to maximize the intramolecular N–H···π interaction.[26] These studies discuss the conformational preference of the p-dopamine monomer in the gas and solution phases as well as the role of the protonated units in the stability of its different rotamers. In a recent study, the influence of different groups on the intermolecular interaction energies of different aromatic molecules, including neutral dopamine, has been studied in addition to the interaction of these molecules with a grapheme surface. It has been shown that T-shaped structural dimers of dopamine are most stable and the stabilities are dominated by the presence of $–NH_2$ interactions with the π-ring due to quadrupole interactions.[27] It is well established that p-dopamine interacts with the dopaminergic receptors where the conformation and noncovalent interactions of p-dopamine play important roles in its key and lock binding with its receptors.[28–30] Earlier studies are mainly focussed on the conformational as well as noncovalent interactions of the monomeric form of p-dopamine in the solution and gas phases. However, in the physiological condition, the aggregated form of p-dopamine exists and its binding with its receptors are highly dependent on the concentrations.[29,31] Hence, understanding of the stability, conformation state and the role of the noncovalent interactions of the aggregated form of p-dopamine in the aqueous medium is important.

In this manuscript, we have studied the concentration dependent change in the UV–Visible spectra of p-dopamine in the aqueous buffer medium (pH = 7.4) to understand the role of the different aggregated forms of p-dopamine in the ground state. Further, the quantum chemical calculation has been performed to understand the energetic, conformational state and the role of noncovalent interactions in the stability of the aggregated p-dopamine in the ground state.

2. Method section

2.1 *Experimental section*

Dopamine hydrochloride (98% purity) was purchased from Sigma-Aldrich. All solutions were freshly prepared in 10 mM Tris-HCl buffer (pH=7.4) and stored at 4 °C. All the experiments were performed at 25 ± 2 °C. UV–Visible measurements were performed using Evolution 201 (Thermo Fisher) spectrophotometer. Fluoromax 4 (HORIBA Scientific) spectrometer was used for the steady state emission measurements. The slit width was kept fixed at 2 nm for all the measurements.

2.2 *Computational section*

We selected two monomeric forms (*gauche* and *trans*) to generate the dimers and trimers of protonated dopamine. Both the *gauche* and *trans*-forms of the side chain of p-dopamine were optimized in the aqueous medium. The notations *gauche* and *trans* were taken from a previous study.[20] The conformers were generated by rotating the dihedral angle of C_{ary}–C_{alk1}–C_{alk2}–N of the molecule. Total, eighteen dimeric and ten trimeric forms of dopamine were found to be stable in the aqueous medium. All the optimizations were done using DFT-B3LYP method with Grimme's D2 dispersion correction and 6-311++G(d,p) basis set.[32] The polarisable continuum model (PCM) has been used to include the solvent (water) effect in the calculations.[33] The frequency calculation for each optimised structure provides only positive values confirming the stable nature of the structure at the potential energy surface. The binding energy has been calculated using Equation 1 and has been corrected for the zero point contribution.[34] The relative population of each conformer has been calculated using equation 2.

$$\Delta E_n(n = 2,3) = E_{(n=2,3)} - nE_{monomer} \quad (1)$$

$$\frac{N_i}{N_j} = e^{(g_j - g_i)/kT} \quad (2)$$

here ΔE_n (n = 2,3) represents the binding energies of dimer and trimers of dopamine, $E_{(n=\ 2,3)}$ depicts the energies of the respective dimer and trimer of dopamine whereas the $E_{monomer}$ shows the minimum energy of the monomer. The N_i and N_j represent the populations of the monomer, dimer and trimer with respect to the most stable form. g_j is the free energy of the species of interest for dimer/trimer whereas g_i is the free energy of the minimum energy structure in that form. Finally, we have calculated the absorption maximum of each optimised structure using the TD-B3LYP method with Grimme's D2 dispersion correction and 6-311++G(d,p) basis set to understand the contribution of the different forms of dopamine in its experimental UV–Visible data. All the calculations

were performed using the G16 suit of programme.[35] To understand the nature of interactions between individual interacting molecules in the dimers and trimers of dopamine in solution phase, the Atoms in Molecules (AIM) analysis was also performed using AIM2000 software, using B3LYP/6-311++G(d,p) method.[36,37]

3. Results and Discussions

Figure 1a shows the concentration dependent UV–Visible spectra of p-dopamine, whereas the change in the peak maxima (λ_{max}) of the UV–Visible spectra with respect to the concentration of p-dopamine is shown in Figure 1b. The λ_{max} of p-dopamine appears at ~265 nm and gets red shifted to ~ 279 nm with further addition of dopamine (Figure 1a). The intensity of the UV–Visible spectra of p-dopamine also increases with its concentration. The change in the λ_{max} of p-dopamine with its concentrations depict that the λ_{max} of p-dopamine gets red shifted monotonically up to ~75 μM and then becomes constant. The change in the λ_{max} and intensity of the UV–Visible spectra of p-dopamine suggest that the dopamine exists in different aggregated forms in the ground state. Further, the concentration dependent emission spectra of p-dopamine (Figure S1, SI) were also measured and it was found that the emission maxima appear at 314 nm which does not show any significant shift with the addition of p-dopamine. The intensity of the emission spectra increases with the addition of p-dopamine and it gets saturated around 75 μM. The change in the emission spectra suggests that the aggregated structure of p-dopamine also exists in the excited state; however, the mode of the interaction of the aggregated form of dopamine in the excited state is different from the ground state.

To probe further into the possible contribution of different aggregated forms of p-dopamine in its UV–Visible spectra, the quantum chemical calculations for several conformers of p-dopamine in its dimer and trimer forms have been performed considering the effect of solvent. Here, we have selected the conformers in which the hydroxyl groups of dopamine remain coplanar with the benzene ring and there is O-H···O-H interaction in the catechol moiety as it has been found to be the most stable arrangement in previous reports.[14,26] The structures of *gauche* (M1) and *trans* (M2) form of monomeric dopamine molecules are shown in Figures 2a and 2b respectively. The C_{ary}–C_{alk1}–C_{alk2}–N dihedral angles are −54.7° and −178.4° for M1 and M2, respectively as taken from a previous study.[20] The energetic data suggests that the M1 is slightly more stable (0.84 kcal mol^{-1}) than M2. The population ratio of M1 to M2 was found to be 76:24, which suggests that the *gauche* form is more populated than the *trans* form. The energetic and population data suggest that both M1 and M2 forms of p-dopamine can exist in the solution. However, the population of the *gauche* form is more than *trans* form. Indeed in an earlier experimental study, it has been found that the population of *gauche* form of p-dopamine is more in the neutral and acidic pH conditions than the basic condition.[24] The *gauche* conformation of the side chain in the gas phase has been predicted to be more stable in this type of 1,2-disubstituted ethane as the amino group can interact favourably with the π ring.[13] Further, we have calculated the λ_{max} of M1 and M2 forms of p-dopamine and it was found to be 257.0 and 255.0 nm, respectively. The λ_{max} of M1 form is closer to the experimental value which also suggests

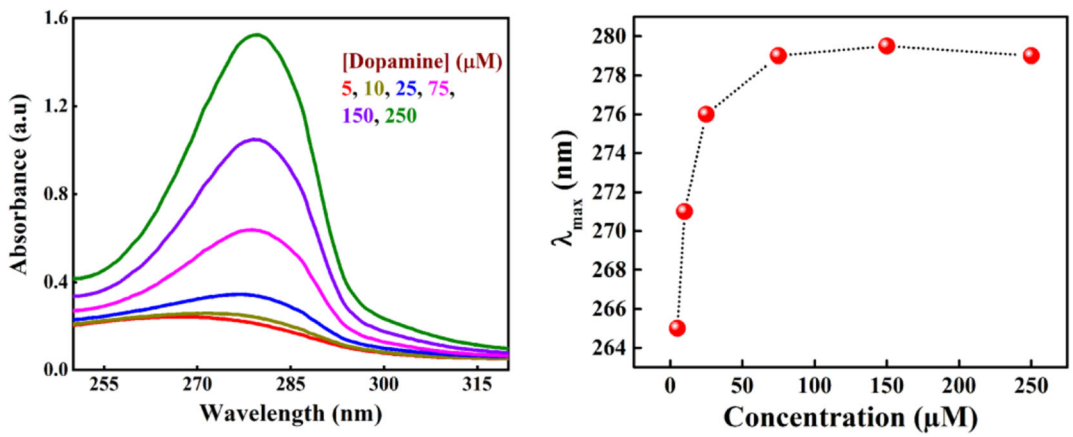

Figure 1. a) UV–visible spectrum of p-dopamine in Tris-HCl buffer with gradually increasing concentrations; b) Plot of the change in the maximum peak positions of p-dopamine with increasing concentrations.

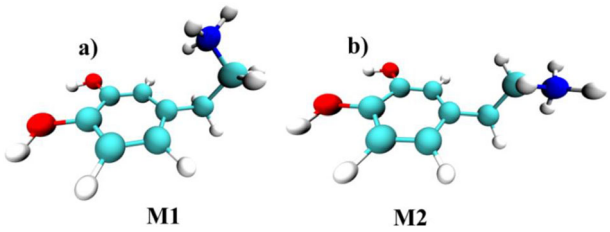

Figure 2. Structures of protonated dopamine monomers having different dihedral angles of C_{ary}-C_{alk1}-C_{alk2}-N a) *gauche* form, M1 b) *trans* form, M2. Colour code used is: C, N, O, H are in cyan, blue, red and white respectively.

dominance of the *gauche* monomeric form of p-dopamine in the aqueous buffer medium of pH = 7.4.

The UV–visible data suggested the role of the higher order of aggregates of p-dopamine in the aqueous buffer medium; hence, we have optimized the different dimeric and trimeric structures of p-dopamine starting from its M1 and M2 monomeric forms. We could find a total of eighteen minimum energy structures of the dimeric form of p-dopamine whose structures are given in Figures 3 (top 10 minimum energy structures) and S2 (remaining eight structures). The structures are arranged in the order of the binding energies (Tables 1 and S1, SI) as D1 has the highest binding energy (10.4 kcal mol^{-1}) and D18 corresponds to the lowest binding energy (4.4 kcal mol^{-1}). The optimized structures of the dimers of the p-dopamine suggest that the most stable structure is T shaped structure in which the -NH_3^+ of p-dopamine interacts with the π electron density of catechol group of other p-dopamine through N–H_3^+···π interaction. The other stabilized structures contain the π···π interaction between the catechol groups of p-dopamine as well as O–H···π interaction. As the calculations have been done in an implicit solvent model (PCM model) instead of vacuum, in the polar medium the dopamine molecules would be expected to interact with the solvent molecules instead of one another. The presence of the NH_3^+ group compensates for this by interacting with the π cloud of dopamine and exposing the basic hydrogens to the solvent. This accounts for the fact that D1 is the most stable structure while D10 is the least stable, even though in the vacuum D10 would have been expected to be most stable due to the double hydrogen bonding. One noticeable observation is that the binding energy of the planar hydrogen bonded dimer of p-dopamine is significantly less than the weakly interacting (having N–H_3^+···π, π···π, O–H···π interactions) complexes. The population calculation also shows that the relative population of the weakly interacted dimeric form of p-dopamine is higher than the planar hydrogen bonded complexes (Figure S4, SI). The energy and population data suggest that the role of the weak interaction is important in the stabilization of the dimeric forms of p-dopamine.

Further, the λ_{max} of the UV–Visible spectra of each structure of the dimers of p-dopamine has been calculated to understand the role of these structures in the experimental UV–Visible spectra (Tables 1 and S1, SI). The λ_{max} of the UV–Visible spectra of the most stable structure is 260.0 nm which is 3 nm red shifted as compared to the monomer data. It is apparent from the calculated λ_{max} of the UV–Visible spectra of the different forms of dimers that the weakly interacted dimers are red shifted as compared to the monomer whereas the planar hydrogen bonded structure shows the λ_{max} similar to the monomer structure. The red shift in the calculated λ_{max} of the weakly interacted (having N–H_3^+···π, π···π, O–H···π interactions) dimer structures of p-dopamine is in well agreement with the experimental trend of the UV–Visible data suggesting that the cation-π (NH_3^+···π), π···π and weakly hydrogen bonded (O-H···π) dimer structures mainly contribute in the UV–Visible spectra of p-dopamine.

Further, we have optimized different forms of trimers of p-dopamine and could locate ten stable structures at the potential energy surface as shown in Figures 4 and S3, SI. The binding energy of each structure is depicted in the Tables 1 and S2, SI. The binding energy of the most stable structure (T1) is 17.3 kcal mol^{-1} whereas the binding energy of the least stable structure (T10) is 8.2 kcal mol^{-1}. The most stable trimer structure (T1) involves the π···π interaction, while the next stable structure (T2) of p-dopamine involves both the π···π and NH_3^+···π interactions as indicated by the presence of bond critical points in the AIM analysis of these structures (Figure 6 and Table S4, SI). T3 structure has mainly the contribution of the π···π interaction between the catecholamine groups of p-dopamine. It is apparent from the structures that the most of the trimers are stabilized by weak noncovalent interactions (N–H_3^+···π, π···π) and the role of the conventional planar hydrogen bonding is not significant. The population analysis shows that the populations of T1 and T2 are significant and the populations of other structures are not so significant which also indicate the role of weak noncovalent interactions (NH_3^+···π, O-H···π, π···π) in the stabilization of the trimer structures of p-dopamine. Further, we have calculated the λ_{max} of each structure (Tables 1 and S2, SI) to compare with the experimental UV–Visible data. In general, the λ_{max} of most of the trimer structures are red shifted as compared to

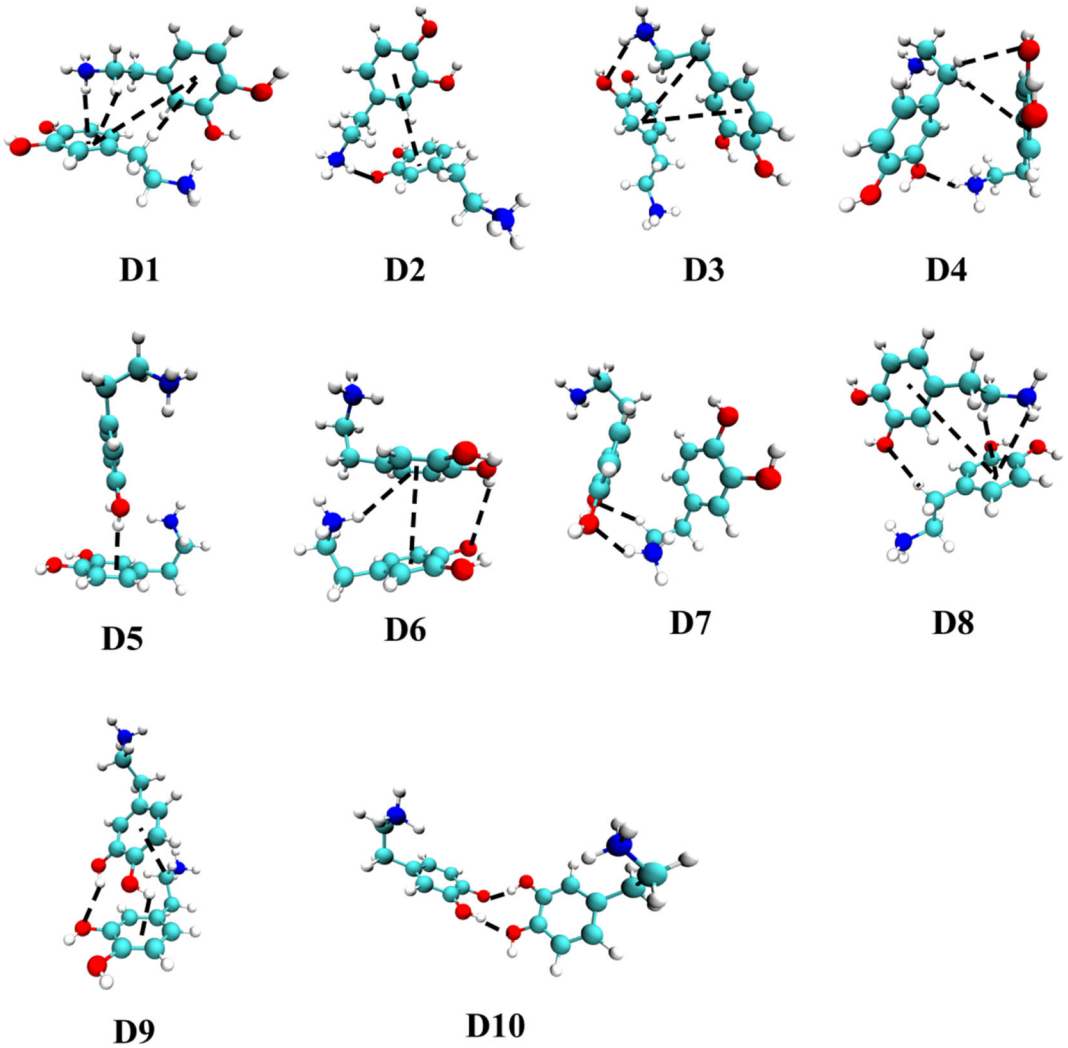

Figure 3. Structures of ten most stable conformers of dopamine dimers. Colour code used is: C, N, O, H are in cyan, blue, red and white respectively. The interactions have been shown with black dashed lines.

Table 1. Binding energy ΔE (kcal mol^{-1}) and λ_{max} (nm) of each structure of the dimer and trimer clusters of p-dopamine.

Structure	M1	M2	D1	D2	D3	D4	D5	D6	D7	D8	D9	D10
ΔE (kcal mol^{-1})	–	–	−10.4	−9.9	−9.7	−8.4	−8.2	−8.0	−7.5	−7.3	−7.1	−6.8
λ_{max} (nm)	257.0	255.0	260.0	262.2	262.1	268.8	260.0	268.0	262.9	267.9	266.7	258.1
			T1		T2		T3		T4		T5	T6
ΔE (kcal mol^{-1})			−17.3		−16.1		−14.4		−13.9		−13.7	−13.1
λ_{max} (nm)			267.7		276.2		267.2		259.8		274.7	269.7

monomer as well as dimer structures. It is apparent from the data that those trimer structures which have more N–H_3^{+}···π interaction (T2 and T9) have more red shifted λ_{max} compared to those species which have π···π and O-H···π interactions. The increase in the red shift of the λ_{max} value with the increase of the cluster size of p-dopamine is in the correlation with the experimental data. The quantum chemical calculations and experimental data suggest that weak noncovalent interactions (N–H_3^{+}···π, π···π and O-H···π interactions) contribute in the aggregation of the p-dopamine in its ground state and the contribution of the higher order of clusters in its UV–Visible spectra increases with the concentration.

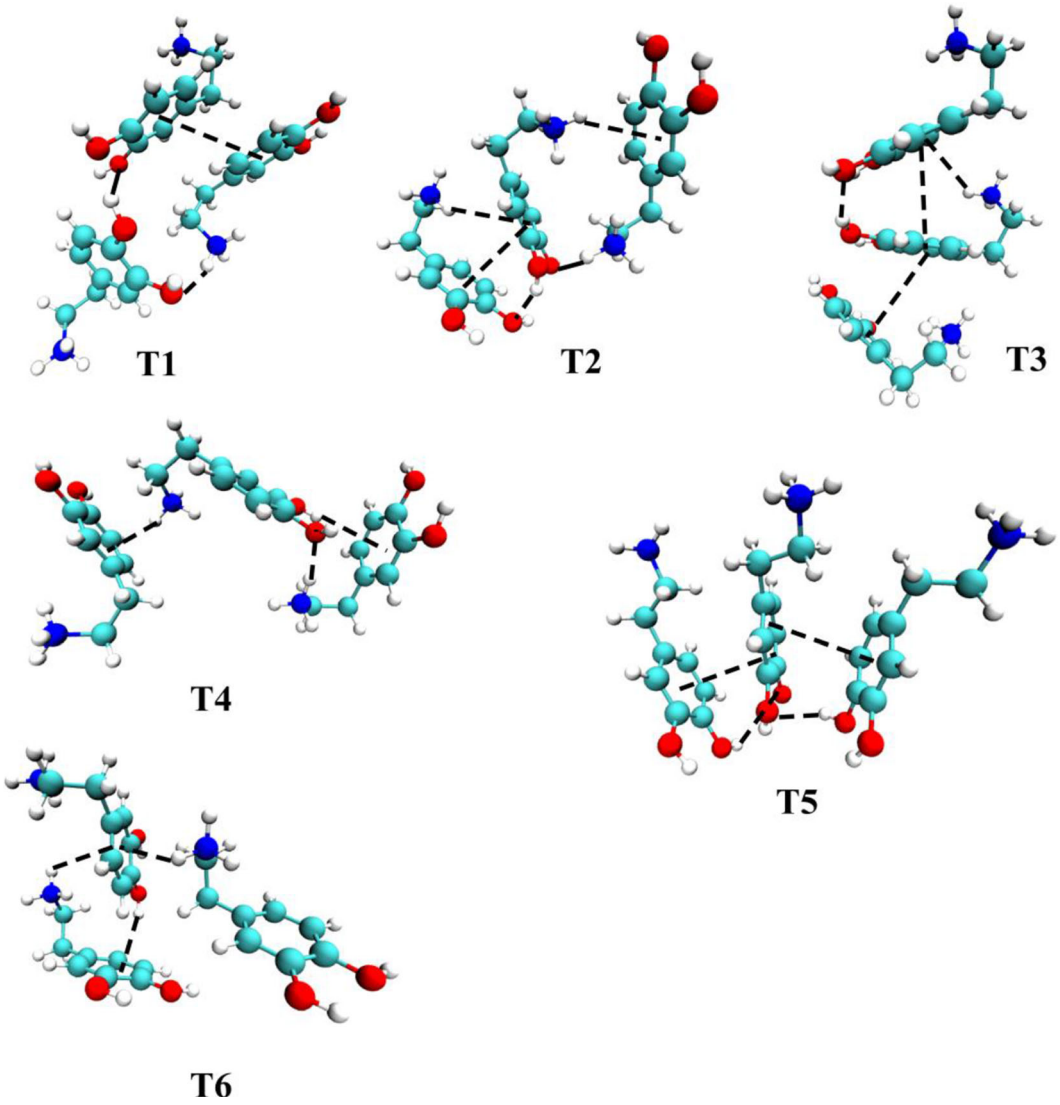

Figure 4. Structures of six most stable conformers of dopamine trimers. Colour code used is: C, N, O, H is in cyan, blue, red and white respectively. The interactions have been shown with black dashed lines.

Finally, we have investigated the nature of weak interactions of the dimer and trimer structures of p-dopamine by doing the AIM calculations of each structure. Figures 5, 6, S5–S7, SI depict the molecular graphs of the electron densities for the different optimized structures of dimers and trimers. The values of the electron density (ρ) , Laplacian (∇^2), total electronic energy (H) and its components, potential energy (V) and local kinetic energy (G) at the bond critical points (BCP) for dimers and trimers are shown in Tables S3 and S4 (SI), respectively. A (3, −1) BCP with a positive Laplacian indicates the presence of noncovalent interactions and a (3, +1) ring critical point (RCP) along with the BCP indicates the presence of a cyclic structure. The topological parameters for all the interactions are in the range of noncovalent interactions.[38,39] D1 shows BCP for several C–H···C, N–H_3^+···C and N–H···O contacts, which show the presence of π···π, cation-π and linear intermolecular hydrogen bonding in the structure. There are (3, +1) BCPs present between the N–H_3^+···C and C–H···C contacts which show the cyclic structure. D2 shows the presence of BCPs for the N–H···O and C–H···C contacts showing the presence of N–H···O and C–H···π contacts. D2 structure does not have the N–H_3^+···π contact like in D1; hence the stabilization of D2 is less than D1. Similar to D2, D3, D4 and D5 depict BCPs for C–H···C and N–H···O contacts but do not possess BCP for N–H_3^+···π contacts. D7 and D10 have the conventional planar hydrogen bonds and do not possess any weak noncovalent interactions like N–H_3^+···π, C–H···π contacts. However, the binding energies of these planar conventional hydrogen bonded structures are lesser than the structure which is

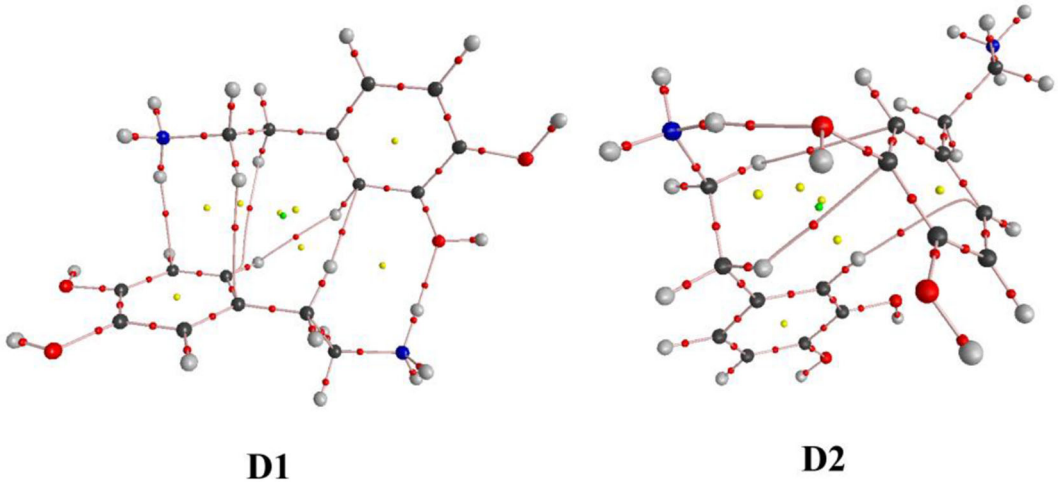

Figure 5. Molecular graphs of the topologies of electron densities for the two most stable dimers of p-dopamine.

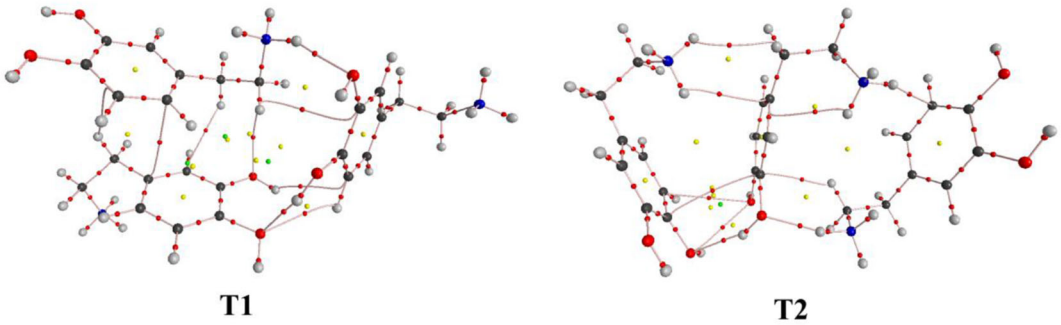

Figure 6. Molecular graphs of the topologies of electron densities for the two most stable trimers of p-dopamine.

hydrogen bonded along with having weak noncovalent interactions, suggesting that noncovalent interactions cooperate the formation of strong hydrogen bonds. Hence, the cooperative effect of the noncovalent interactions along with the hydrogen bonding is important in the stabilization of the p-dopamine dimers. The molecular graphs of all the trimer structures have noncovalent interactions N–$H_3^{+\cdots}\pi$, C–H$^{\cdots}\pi$, $\pi^{\cdots}\pi$ along with the N–H$^{\cdots}$O hydrogen bond. We could not find any trimer structure which has the pure conventional N–H$^{\cdots}$O hydrogen bond without the contribution from the noncovalent interactions suggesting the importance of the weak noncovalent interactions in the stabilization of the higher order of clusters of p-dopamine.

4. Conclusions

The intensity of the UV–Visible spectra of p-dopamine increases and shows the red shift with the increasing concentrations of p-dopamine. The change in the UV–Visible spectra of p-dopamine suggests that the aggregation of p-dopamine takes place in the aqueous medium. The quantum chemical calculation and AIM analysis of the different dimer and trimer structures of p-dopamine suggest the presence of N–$H_3^{+\cdots}\pi$, C–H$^{\cdots}\pi$, $\pi^{\cdots}\pi$ weak interactions along with the conventional N–H$^{\cdots}$O hydrogen bond. The calculated peak positions of the UV–Visible spectra of different clusters show that the higher order clusters show red shifted peak position compared to the monomer and the red shifted peak is more evident in the clusters having noncovalent interactions. These studies show that the role of the noncovalent interaction is important in the stabilization of the aggregated form of the p-dopamine.

Supplementary Information (SI)

Emission spectra of p-dopamine in buffer, structures of the less stable dimer and trimer structures of p-dopamine, the binding energies and λ_{max} of the less stable structures, the population analysis of the less stable dimers and trimers, the

molecular topology graphs of the electron densities of the less stable structures and the values of the parameters for the bond critical points for all the dimer and trimer structures of p-dopamine, the optimised coordinates of the monomers, D1 and T1 of p-dopamine. Supplementary information is available at www.ias.ac.in/chemsci

References

1. Korshunov K S, Blakemore L J and Trombley P Q 2017 Dopamine: a modulator of circadian rhythms in the central nervous system *Front. Cell. Neurosci.* **11** 91
2. Jaber M, Robinson S W, Missale C and Caron M G 1996 Dopamine receptors and brain function *Neuropharmacology* **35** 1503
3. Lot T Y 1993 Mechanisms of action of dopamine in the peripheral nervous system of chicks and rats *J. Pharm. Pharmacol.* **45** 896
4. Rubí B and Maechler P 2010 Minireview: new roles for peripheral dopamine on metabolic control and tumor growth: let's seek the balance *Endocrinology* **151** 5570
5. Murty V P, Tompary A, Adcock R A and Davachi L 2017 Selectivity in postencoding connectivity with high-level visual cortex is associated with reward-motivated memory *J. Neurosci.* **37** 537
6. Alcaro A, Huber R and Panksepp J 2007 Behavioral functions of the mesolimbic dopaminergic system: an affective neuroethological perspective *Brain Res. Rev.* **56** 283
7. Marsden C A 2006 Dopamine: the rewarding years *Br. J. Pharmacol.* **147(Suppl 1)** S136
8. Thorp J, Clewett D and Riegel M 2020 Two routes to incidental memory under arousal: dopamine and norepinephrine *J. Neurosci.* **40** 1790
9. Burbulla L F, Song P, Mazzulli J R, Zampese E, Wong Y C, Jeon S, et al. 2017 Dopamine oxidation mediates mitochondrial and lysosomal dysfunction in Parkinson's disease *Science* **357** 1255
10. Surmeier D J, Obeso J A and Halliday G M 2017 Selective neuronal vulnerability in Parkinson disease *Nat. Rev. Neurosci.* **18** 101
11. Meisenzahl E M, Schmitt G J, Scheuerecker J and Möller H J 2007 The role of dopamine for the pathophysiology of schizophrenia *Int. Rev. Psychiatry* **19** 337
12. Cabezas C, Peña I, López J C and Alonso J L 2013 Seven conformers of neutral dopamine revealed in the gas phase *J. Phys. Chem. Lett.* **4** 486
13. Urban J J, Cronin C W, Roberts R R and Famini G R 1997 Conformational preferences of 2-phenethylamines: A computational study of substituent and solvent effects on the intramolecular amine−aryl interactions in charged and neutral 2-phenethylamines *J. Am. Chem. Soc.* **119** 12292
14. Fausto R, Ribeiro M J S and de Lima J J P 1999 A molecular orbital study on the conformational properties of dopamine [1,2-benzenediol-4(2-aminoethyl)] and dopamine cation *J. Mol. Struct.* **484** 181
15. Callear S K, Johnston A, McLain S E and Imberti S 2015 Conformation and interactions of dopamine hydrochloride in solution *J. Chem. Phys.* **142** 014502
16. Bustard T M and Egan R S 1971 The conformation of dopamine hydrochloride *Tetrahedron* **27** 4457
17. Bergin R and Carlstrom D 1968 The structure of the catecholamines: II: The crystal structure of dopamine hydrochloride *Acta Cryst. B* **24** 1506
18. Giesecke J 1980 Refinement of the structure of dopamine hydrochloride *Acta Cryst. B* **36** 178
19. Park S, Lee N S, Lee S J B and o T K C S, 2000 Vibrational analysis of dopamine neutral base based on density functional force field *Bull. Korean Chem. Soc.* **21** 1035
20. Lagutschenkov A, Langer J, Berden G, Oomens J and Dopfer O 2011 Infrared spectra of protonated neurotransmitters: dopamine *Phys. Chem. Chem. Phys.* **13** 2815
21. Zhai C, Ma H, Sun F, Li L and Song A 2016 Experimental and theoretical study on the interaction of dopamine hydrochloride with H2O *J. Mol. Liq.* **215** 481
22. Berfield J L, Wang L C and Reith M E 1999 Which form of dopamine is the substrate for the human dopamine transporter: the cationic or the uncharged species? *J. Biol. Chem.* **274** 4876
23. Granot J 1976 Nmr studies of catecholamines. Acid dissociation equilibria in aqueous solutions *FEBS Lett.* **67** 271
24. Solmajer P, Kocjan D and Solmajer T 1983 Conformational study of catecholamines in solution *Z. Naturforsch. C* **38** 758
25. Alagona G and Ghio C 1996 The effect of intramolecular H-bonds on the aqueous solution continuum description of the N-protonated form of dopamine *Chem. Phys.* **204** 239
26. Nagy P I, Alagona G and Ghio C 1999 Theoretical studies on the conformation of protonated dopamine in the gas phase and in aqueous solution *J. Am. Chem. Soc.* **121** 4804
27. de Moraes E E, Tonel M Z, Fagan S B and Barbosa M C 2019 Density functional theory study of π-aromatic interaction of benzene, phenol, catechol, dopamine isolated dimers and adsorbed on graphene surface *J. Mol. Model.* **25** 302
28. Durdagi S, Salmas R E, Stein M, Yurtsever M and Seeman P 2016 Binding interactions of dopamine and apomorphine in D2high and D2low states of human dopamine D2 receptor using computational and experimental techniques *ACS Chem. Neurosci.* **7** 185
29. Bueschbell B, Barreto C A V, Preto A J, Schiedel A C and Moreira I S 2019 A complete assessment of dopamine receptor- ligand interactions through computational methods *Molecules* **24** 1196
30. Floresca C Z and Schetz J A 2004 Dopamine receptor microdomains involved in molecular recognition and the regulation of drug affinity and function *J. Recept. Signal Transduct. Res.* **24** 207
31. Salmas R E, Yurtsever M, Stein M and Durdagi S 2015 Modeling and protein engineering studies of active and inactive states of human dopamine D2 receptor (D2R)

and investigation of drug/receptor interactions *Mol. Divers.* **19** 321
32. Grimme S 2006 Semiempirical GGA-type density functional constructed with a long-range dispersion correction *J. Comput. Chem.* **27** 1787
33. Miertuš S, Scrocco E and Tomasi J 1981 Electrostatic interaction of a solute with a continuum. A direct utilizaion of ab initio molecular potentials for the prevision of solvent effects *Chem. Phys.* **55** 117
34. Dubinets N O, Safonov A A and Bagaturyants A A 2016 Structures and binding energies of the naphthalene dimer in its ground and excited states *J. Phys. Chem. A* **120** 2779
35. Frisch M J, Trucks G W, Schlegel H B, Scuseria G E, Robb M A, Cheeseman J R, Scalmani G, Barone V, Petersson G A, Nakatsuji H, Li X, Caricato M, Marenich A V, Bloino J, Janesko B G, Gomperts R, Mennucci B, Hratchian H P, Ortiz J V, Izmaylov A F, Sonnenberg J L, Williams, Ding F, Lipparini F, Egidi F, Goings J, Peng B, Petrone A, Henderson T, Ranasinghe D, Zakrzewski V G, Gao J, Rega N, Zheng G, Liang W, Hada M, Ehara M, Toyota K, Fukuda R, Hasegawa J, Ishida M, Nakajima T, Honda Y, Kitao O, Nakai H, Vreven T, Throssell K, Montgomery Jr J A, Peralta J E, Ogliaro F, Bearpark M J, Heyd J J, Brothers E N, Kudin K N, Staroverov V N, Keith T A, Kobayashi R, Normand J, Raghavachari K, Rendell A P, Burant J C, Iyengar S S, Tomasi J, Cossi M, Millam J M, Klene M, Adamo C, Cammi R, Ochterski J W, Martin R L, Morokuma K, Farkas O, Foresman J B and Fox D J 2016 Gaussian 16 Rev. C.01 Wallingford CT
36. Bader R F W 1990 *Atoms in Molecules: A Quantum Theory* (Oxford: Clarendon Press)
37. AIM2000 2001 *J. Comput. Chem.* **22** 545
38. Koch U and Popelier P L A 1995 Characterization of C-H-O hydrogen bonds on the basis of the charge density *J. Phys. Chem.* **99** 9747
39. Popelier P L A 1998 Characterization of a dihydrogen bond on the basis of the electron density *J. Phys. Chem. A* **102** 1873